Characterisation of a Retro-Fit Engine Intake Water Doping Device for Improved Urban Air Quality

A thesis submitted for the degree of Masters of Science in

Engineering with Innovation and Entrepreneurship

by

Seifeldin Mohamed Said Mattar, BEng (Hons)

Department of Mechanical Engineering University College London

I, Seifeldin Mohamed Said Mattar, confirm that the work presented in this thesis is my own. Where information has been derived from other sources, I confirm that this has been indicated in the thesis.

September 2018

Word Count: 11989

Abstract

A novel intake manifold water injection device that has emerged for its special abilities in emission reductions is the Econokit. The Econokits performance in reducing emissions has varied however and the gas outputs that it injects into the intake manifold are yet to be known. Therefore, this project characterises the Econokit device to understand its gas outputs and to understand why its performance varies from one engine to the other.

An experimental bench was set up to simulate the same conditions that the Econokit experiences in a car engine. These conditions were varied and using a humidity sensor and gas analyser the gas composition of the Econokits output was analysed. From the results it was seen that as the bubbler temperature was increased, the water content in the Econokit output air flow also increased. It was also seen that the Econokits reactor does indeed change the air flow composition. When high temperatures were applied to the reactor, from 200-450 °C, both CO, up to 192 ppm, and CO_2, up to 5100 ppm

Acknowledgments

I would like to thank and acknowledge my supervisor, Dr Paul Hellier, for his unparalleled guidance and support throughout the entirety of this project. I am also grateful for Dr Hellier and UCL for providing such a challenging and exiting project and for allowing me to use the experimental equipment required for the completion of the project.

Table of Contents

Nomenclature

CI	Compression Ignition
CO	Carbon Monoxide
CO_2	Carbon Dioxide
CV	Co-efficient of Variance
DI	Direct Injection
Dr	Dilution Ratio
DWI	Direct Water Injection
EGR	Exhaust Gas Recirculation
H_2O	Water
HFO	Heavy Fuel Oil
HC	Hydrocarbon
IMWI	Intake Manifold Water Injection
IMI	Intake Manifold Injection
LFO	Light Fuel Oil
N_2	Nitrogen
NO	Nitric Oxide
NOx	Nitrogen Oxides
PM	Particulate Matter
SD	Standard Deviation
SI	Spark Ignition
SO_2	Sulphur Dioxide
WI	Water Injection

List of Tables

List of Figures

02[( )] TJ.....ETBT1 0 0 1 522.1 530.47 02[( )] TJETBT1 0 0 1 339.07 530.47 02[( )] TJ23ET EMC /P 4MCID 19/La

1 Introduction

Greenhouse gas emissions and harmful air pollutants represent an ongoing, evolving threat on worldwide human health and well-being. Emission levels have increased by 80% since 1970 [International Energy Agency 12], causing; a constant increase in global warming, smog and ozone air pollution and most importantly an overall deterioration in average human health and average human life expectancy [Government of Canada 2017; What's Your Impact 18]. Transportation presents a major source of greenhouse gas emissions, it is the largest contributor to harmful emissions in the UK at 26% of total greenhouse gas emissions [Gabbattis 18], as well as the largest contributor in the US at 28% of total emissions [EPA 18]. On the global scale, emissions from transportation accounts to 14% of all greenhouse gas emissions [EPA 18].

Emissions from transportation, produced from petrol and diesel engines are particularly dangerous on human health. Harmful emissions from transportation include; carbon monoxide, nitrogen oxides, particulate matter and hydrocarbons [Vehicle Certificate Agency 18]. These gases, if inhaled, will block the passage of oxygen from the heart and the brain, they would also result in lung irritation and respiratory illness [Vehicle Certificate Agency 18; Union of Concerned Scientists 18]. Particulate matter in particular can also penetrate deep into the lungs and cause deaths in many occasions. In the UK alone for example, 29000 deaths a year are credited to particulate matter pollution [Public Health England 14].

Measures are therefore being taken to try and limit the level of emissions. The introduction of electric vehicles has been a major factor in attempts to reduce emission levels. Electric vehicles can emit less than half the amount of emissions that are emitted from petrol and diesel engines [Neslen 18]. However, electric vehicles only account to a very small percentage of total vehicles in use, for example, in the UK, in 2018, only about 0.53% of total vehicles in use will be electric [Department for Transport 18; Hull 18]. The percentage of electrical vehicles in use is even lower in the less developed countries [Statista 2018], and only by 2040 is electric vehicles expected to be the primary source of transportation [Leahy 18].

Consequently, in an attempt to lower emission levels, governments have been introducing emission standards to limit the maximum amount of emissions from vehicles [Government of Canada, 2018]. To meet the new government emission standards, new techniques and innovations are constantly being studied and developed. A technique that has been proven to reduce harmful gas emissions in vehicles is water injection. Water injection has proven to cause a decrease in levels of emissions from exhausts when applied to engines

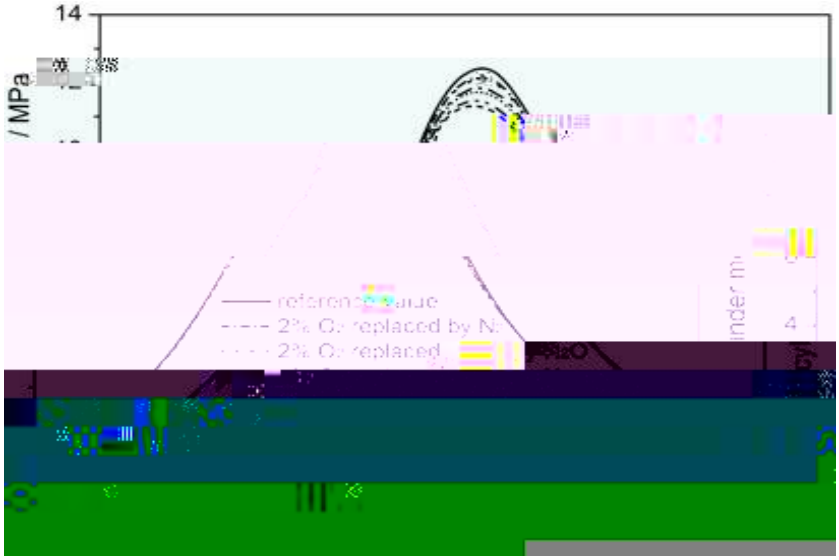

Figure 4. In-cylinder pressure vs crank angle for different intake

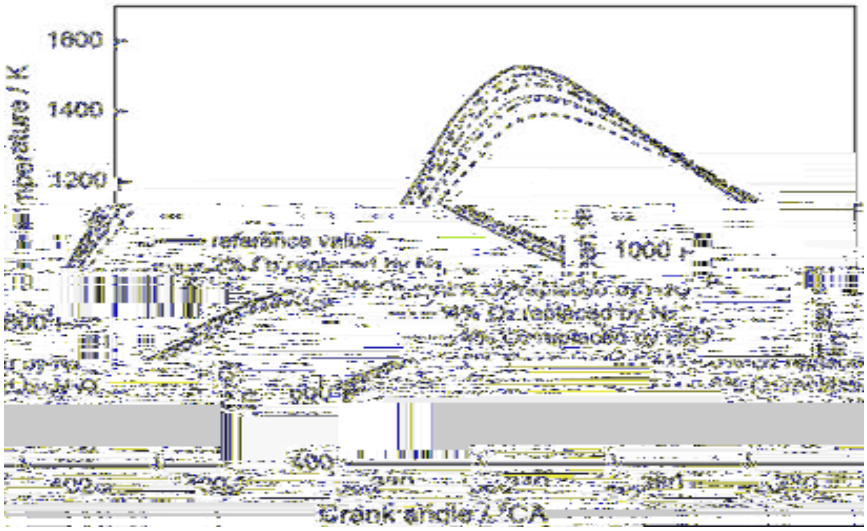

From Ma et al [2007] results of engine NOx emissions at different inlet charge compositions, shown in figure 6 below, it can be seen that although both water and nitrogen injection induce the dilution effect, as discussed above, the injection of water has the largest effect on reducing NOx emissions. This is due to the chemical and thermal effects of water injection that have been discussed earlier. Since the dilution effect has the largest influence on NOx emissions as concluded by Tauzia et al [2009] and Farag et al [2017], only a small, but important difference in reduction in emissions is caused by using water instead of nitrogen in the inlet charge, as seen in figure 6 below.

3.3 Effect of IMWI on Emission Reduction

This section carefully studies and analyses the effect of using IMWI on each of the different exhaust emissions.

3.3.1 Effect of IMWI on NOx Emissions

Through reducing the in-cylinder pressure and temperature as well as through the thermal, chemical and dilution effects discussed in section 3.2.2 above, IMWI can drastically reduce the engines NOx emissions [Ma et al 14]. Upon testing IMWI on a hydrogen-fuelled engine, Subramanian et al [2007] were able to realise a 32% reduction in NO emissions without any losses in break thermal efficiency. Tauzia et al [2009] also experienced up to 50% reductions in NOx emission when they applied the IMWI system on a direct injection diesel engine.

The effect of IMWI on NOx emissions however depends significantly on the rate of water injection. To analyse the effect of the rate of water injection on engine NOx emissions, Tauzia et al [2009] applied an IMWI system onto a direct injection diesel engine, NOx emissions were recorded at different water injection rates for the diesel engine operating under four different loads, **a-**

shown on figure 7 below. As seen in figure 7, the results obtained by Tauzia et al [2009] agree with Subramanian et al [2007] in that using IMWI results in a significant reduction in NOx emissions. The reduction was observed for all 4 engine loads, with load **a** being the lowest engine load and load **d** being the highest (operating loads used by Tauzia et al [2009]

by Babu et al [2015], shown in figure 8 below, it can be seen that IMWI decreases NOx emissions at all engine speeds. More interestingly, it is seen that IMWI has the highest effect on NOx emissions when the engine is operating at medium speeds. The highest reductions in NOx emissions were observed by Babu et al [2015] when the engine was operating at speeds between 3000 rpm and 4500 rpm.

Another factor that influences the performance of an IMWI system on NOx emission reduction is the combustion phasing [Arruga et al 17]. Arruga et al [2017] applied IMWI on a spark ignition, NOx emissions were then observed as the combustion phasing was varied. Combustion phasing, which is the time in the engine cycle while combustion occurs [Wildhaber 11], was varied by Arruga et al [2017] through

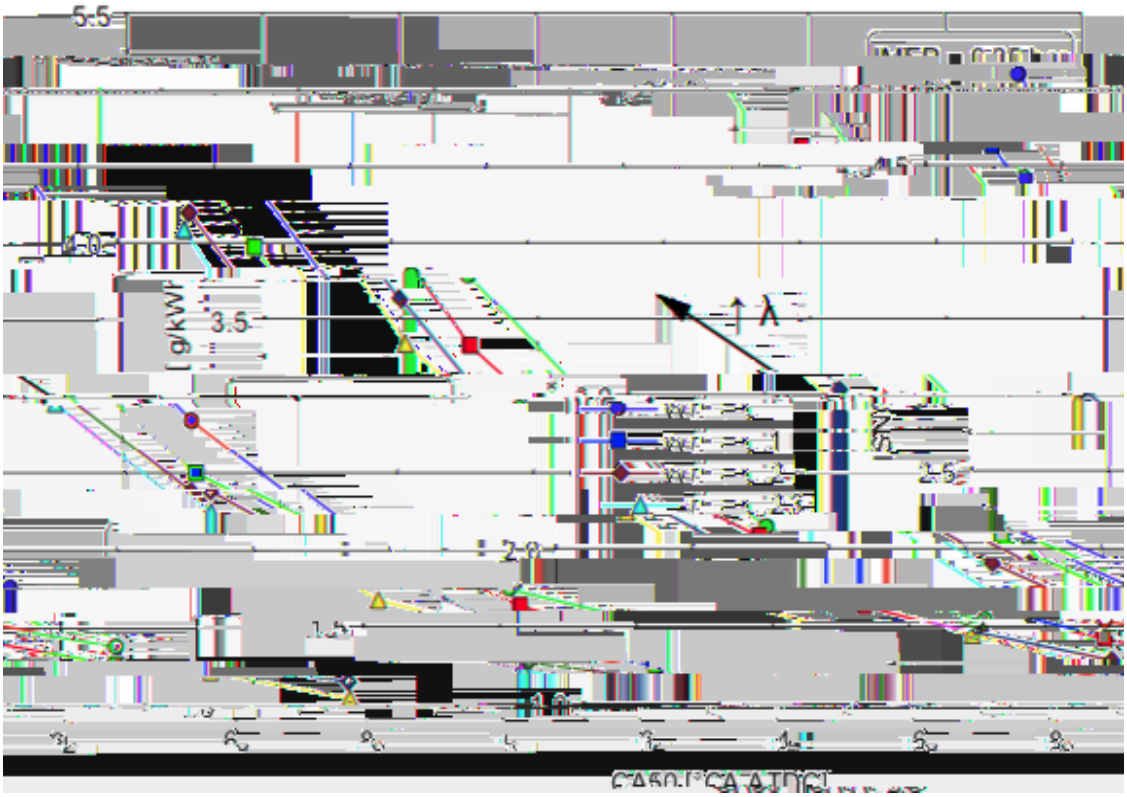

Figure 9. NOx emissions vs combustion phasing CA50 [Arruga et al 2017].

3.3.2 Effect of IMWI on CO Emissions

Intake manifold water injection also has an effect on the CO emissions of an engine. As with NOx emissions, the effect of IMWI on the CO emissions also depends on the engine load, engine speed and rate of water injection.

IMWI was applied onto a compression ignition engine by Tesfa et al [2012] to analyse the effect it has on the engineôs CO emissions. CO emission levels were measured by Tesfa et al [2012] for the CI engine operating under two different loads while the engine speed was varied as two different water injection rates were used. From the results obtained by Tesfa et al [2012], presented in figures 10 a-d below, it can be concluded that IMWI has a negative effect on CO emissions. When IMWI was added to the CI engine, the CO emissions increased. The increase in CO emissions were also seen to increase as the water injection rate increased, as seen in figures 10 a-d. This is because, as explained earlier, the injection of water results in a reduction in pre-combustion temperature, although the reduction in pre-combustion temperature reduces the NOx formation as seen in section 3.3.1 above, it does the contrary with CO emissions [Tesfa et al 12]. As the combustion temperatures decrease,

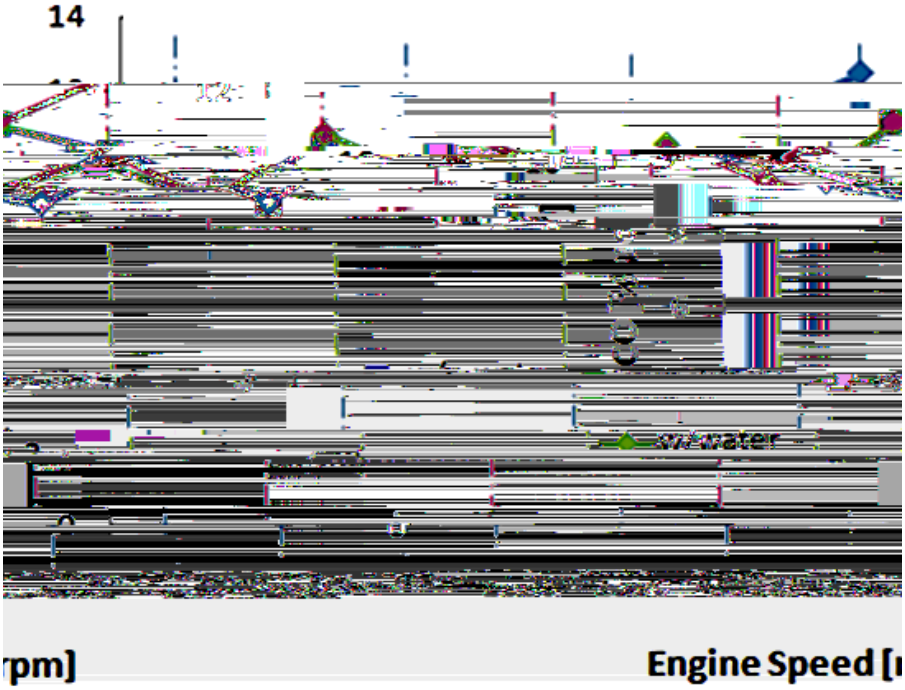

Figure 11. CO emission vs engine speed with and without IMWI for a SI engine [Babu et al 2015]

Overall, as seen, in most occasions IMWI results in an increase in CO emissions, however not always, as IMWIôs effect on CO emissions depends on, as discussed above, WI rate, engine type, engine speed and engine Load.

3.3.3 Effect of IMWI on PM Emissions

IMWI also has a huge influence on particulate matter emission. In most occasions, applying water injection results in an increase in PM emissions [Farag et al 17; Kettner et al 16; Tauzia, Maiboom and Shah 10]. This is because, as explained earlier, water injection results in a reduction in temperature. A reduction in temperature limits soot oxidation which in turn results in more PM exiting into the atmosphere from the engine exhaust [Tauzia, Maiboom and Shah 10].

To understand the effect of IMWI on PM emissions, Tauzia et al [2009] applied an IMWI system onto a DI diesel engine. PM emissions were observed for four different engine loads **a-d**, **a** being the lowest load and **d** the highest, as the water injection rate was varied. Results were also compared with the effect of EGR on PM emissions when added onto the same engine. From the results observed by Tauzia et al [2009], shown in figure 12 below, it can be seen that IMWI increased the PM emissions for the higher loads **b**, **c** and **d** (engine loads are shown in appendix 2). As seen in figure 12 below, as the operating load of an engine is

higher, IMWI causes a larger percentage increase in PM emissions. This is because at higher loads the engine temperature is higher, WI causes a larger temperature reduction when the engine temperature is already at a high level, this results in, as explained, less soot oxidising and so more PM exiting from the exhaust [Tauzia, Maiboom and Shah 10]. Another reason as to why IMWI causes an increase in PM emissions is that IMWI also affects the air to fuel ratio [Tauzia, Maiboom and Shah 10]. A slight decrease in the air to fuel ratio, of about 5-7% was observed by Tauzia et al [2009] when the IMWI wa

Contrary to operating loads **b**, **c** and **d**, when the engine was operating under the lower load, load **a**, the PM emissions obtained by Tauzia et al [2009]

Mr. Alan Cooper [2018] an innovator in the field of IMWI and an Econokit user has claimed that, when the reactor is subjected to elevated temperatures 200 ï 450 C°, it changes the gas composition [Cooper 18]. He also claims that the Sabatier reaction occurs within these temperatures and that methane is produced [Cooper 18].

3.5 Sabatier Reaction

The Sabatier reaction involves the reaction of carbon dioxide with hydrogen at high temperatures, between 300-400 C° in the presence of a nickel catalyst to produce methane and water [Frontera et al 17].

There are two main reactions involved with the Sabatier reaction [Frontera et al 17], these are:

$$4H_{2j}+{}_jCO_{2_j}\ddot{Y}\,{}_jCH_{4j}+{}_j2H_2O \quad (1)$$

$$3H_{2j}+{}_jCO_j\ddot{Y}\,{}_jCH_{4j}+{}_jH_2O \quad (2)$$

With the side reaction of:

$$H_{2j\ 8} \quad \text{Ч} \quad \text{ժ} \quad \text{Ծ}\ {}_6 \quad \text{ॐ}$$

as the under-

After drilling the holes, the bubbler was filled, and using tape, it was placed in the middle of the ABS enclosure, as shown in figure 15 below.

To characterise the effect of the engine bay temperature on the bubbler and on the Econokits performance, the temperature inside of the enclosure was varied. To vary the temperature, a

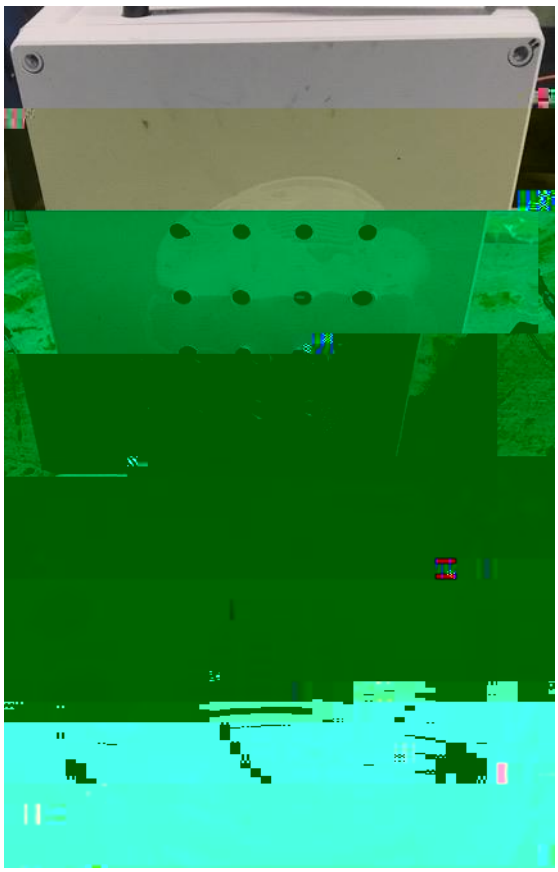

Figure 16. Heater fan subjected onto ABS

This set-up for the bubbler allowed the temperature of the bubblerôs ABS enclosure, which acts as the area under the vehicleôs bonnet, to be varied using the heater fan, while the temperatures is simultaneously being measured using the thermocouple reader.

4.1.2 Catalytic Reactor Set-Up

The reactor has a huge influence on the Econokits performance. It is where the water is polarised and where the gas composition is expected to change. The reactor is placed on the hottest part of the car engine, the exhaust manifold. The performance of the reactor depends significantly on its temperature. The exhaust manifold temperature however varies from one engine to another which means that the reactor temperature and performance also varies when it is applied on different engines. To characterise the effect of the reactor temperature on the Econokits outputs, the reactor was set up on the test bench in a way that allows its temperature to both be varied and measured simultaneously.

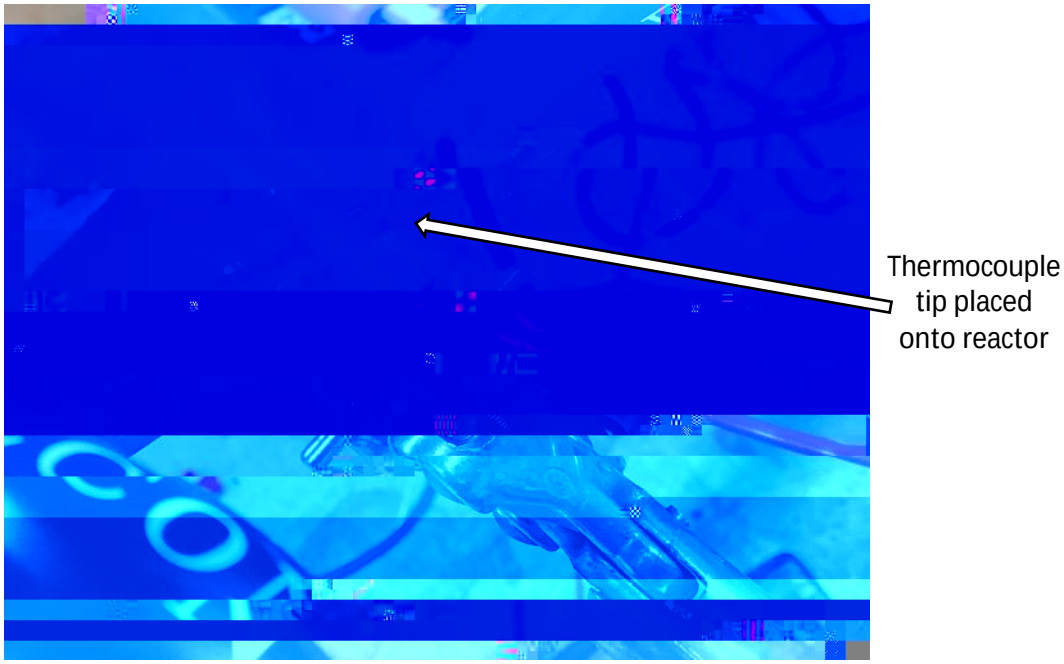

Figure 19. Thermocouple placed onto

The Steinel heat gun could only however get the reactorôs temperature up to 220 CÁ, where the temperatures for the tests were required to go up to 450 C°. To increase the reactors temperature further and reach the 450 C° mark, a blowtorch was subjected onto the reactor, as shown in figure 20 below.

4.1.3 Diffuser Set-Up

The diffuser, which is placed into the intake manifold, creates the air flow for the Econokit and injects the Econokits products into the intake manifold. When placed into the intake manifold, using the pressure difference that it creates, the venturi tube diffuser pulls air through the bubbler, through the reactor and into the intake manifold. To simulate the same function of the diffuser, a suction pump was used in the bench set-up. The suction pump was connected at the end of the Econokit setup and was used to act as the diffuser in pulling air through the Econokit device. The air flow rate created by the suction pump was kept constant and was not varied throughout all tests. The suction pump and its connection are shown in figure 21 below.

Figure 21. Suction pump used to stimulate air flow through the Econokit device a) connection between suction pump and Econokit set-up b).

4.1.4 Humidity Sensor Set-Up

To understand and characterise the Econokit device, a humidity sensor was used to measure the water content at the different operating conditions. A TE Connectivity HM1500LF Relative Humidity Sensor was added to the set-up and placed between the bubbler, in its enclosure, and the reactor. To add the humidity sensor to the set-up and get continuous humidity readings without hampering the air flow, the hose connecting the bubbler to the reactor was cut in half and an insertion for the sensor was added in-between. To create the humidity sensor insertion, two pieces of 20 cm long, 22 mm diameter copper pipes were connected together using a brass tee compression fitting, the third connection of the tee fitting was used to insert the humidity sensor. The humidity sensor diameter however is only 12 mm whereas the diameter of the tee fitting in which it would be inserted into is 22 mm.

Upon installing the humidity sensor in the test bench set-up, the sensor was connected to a Metrix MX23 multimeter and a 5V voltage was supplied to it. Continuous readings of the Econokit air flow humidity was then observed as a voltage value from the multimeter. Using the voltage readings, the relative humidity of the air flow was figured by using the voltage to relative humidity reference chart and reference table from the data sheet provided by TE Connectivity which is shown in appendix 3.

4


Enclosure with Bubbler
Thermocouple Reader
Multimeter

5 Results and Discussion

In this section, results are given for; the effect of bubbler temperature on the amount and rate of water injected by the Econokit, and the effect of reactor temperature on the gas composition of the Econokits outputs. The results obtained from each of tests are also discussed and analysed in this section.

5.1 Characterisation of Bubbler Temperature to Water Vapour Content

As mentioned earlier, this test was carried out by varying the temperature of the ABS enclosure, which represents the under-bonnet area in a vehicle, from room temperature, 23 °C, to 65 °C. Readings of humidity, or water vapour content, were then taken from the multimeter as voltage values at temperature intervals of 2 °C. The test was run multiple times and the readings for three runs is shown in Table 1 below.

Enclosure Temperature (C°)	Run 1	Run 2	Run 3
23	2792	2856	2982
25	2832	2869	

Table 1 above shows the readings of the relative humidity of the air flow in the Econokit set-up as the temperature of the enclosure was varied for three different runs. The readings were taken in mV off of the multimeter. To get the relative humidity % from the voltage values, the reference graphs and table provided by TEConnectivity, shown in appendix 3, were used.

To accurately find the relative humidity, along with the table and graphs mentioned above, the following equation, which was also provided in the data sheet for the sensor, was used:

$$(\%) = 0.03892 \quad (\quad) - 42.017 \qquad (4)$$

Using the equation given, the relative humidity of the Econokit air flow at the different enclosure temperatures was calculated and is given in table 2 below.

Enclosure Temperature (C°)	Run 1	Run 2	Run 3
23	66.65	69.14	74.04
25	68.20	69.64	75.21
27	70.03	70.11	77.35
29	70.23	70.54	77.78
31	70.07	70.77	78.09
33	70.35	70.89	78.83
35	70.46	72.37	79.72

As seen in table 4 and figure 27 above, the temperature of the enclosure, which represents the temperature of the under-bonnet area in a vehicle, has a huge effect on the amount and rate of water being injected by the Econokit. Remarkably, what was seen is that for all three runs, the mass of water per m^3 of air being injected increased significantly from enclosure temperature 23 °C to enclosure temperature 65 °C. Where for the three runs, the mass of water per m^3

The main reason for the increase in water vapour content in the air flow as the enclosure temperature, or engine bay temperature, is increased is attributed to the fact that when the enclosure or engine bay temperature is higher, the temperature of the water inside of the

the summary in table 5 below, for a given range of reactor temperatures, the range of values of SD and CV calculated for each of the temperatures in that range is given.

Table 5. Summary of standard deviation and co-efficient of variance for CO_2 concentration in output air flow at each reactor temperature.

From table 5 above, it can be seen that for low reactor temperatures, the standard deviation and the coefficient of variance for the CO_2 output from the mean CO_2 output, shown in figure 28, is high. This means that the CO_2 output at the low reactor temperatures can vary from the mean given in figure 28, however the variation would have little significance as at the low reactor temperatures the CO_2 output is already low and insignificant in affecting engine emissions and with any deviation in the concentration of CO_2 at these low reactor temperatures, the CO

As seen from figure 29 above, at elevated temperatures, the reactor produces CO gas. From temperatures of 220 °C, 215 °C and 205 °C for Run 1,2 and 3 respectively, CO was detected in the output gas composition. As the temperature of the reactor was increased, the CO concentration was also seen to increase. For Run 1 the maximum concentration of CO obtained, 185 ppm, was achieved at reactor temperature 425 °C. For Run 2 and 3 however the maximum concentration of CO obtained was 192 and 180 ppm and were obtained at reactor temperature 405 °C and 380 °C respectively. For the three runs it was seen that upon reaching the maximum concentration of CO at the reactor temperatures mentioned, any further increase in reactor temperature would act to reduce the CO concentration in the output air flow composition. As explained in section 5.2.1 above, the reason for the CO production in the Econokits reactor, is the same as that for the CO_2 production, which is at

As seen from table 6 above, for low reactor temperatures, the CV is high. The SD is however very low at the lower reactor temperatures and indicates that the even if the CO concentration at the low temperatures can vary considerably from the mean of CO output sown in figure 29 above, the amount of which the CO will vary will not have a significant influence on the effect of the injected CO. For higher reactor temperatures, where the CO production and concentration is also higher, it is seen from table 6 that the SD for CO outputs is also higher. The CV however is lower at the higher reactor temperatures and indicates that at these temperatures the CO produced and injected would be similar to that shown on the mean curve in figure 29 above.

Overall from the results of CO concentration, is seen that if the reactor temperature is between 390 ï 430 °C, it can produce CO at a concentration of up to 192 ppm. However, this amount indicates that the CO produced by the reactor, which is then injected into the intake manifold, is insufficient for it to have an effect on emissions in the same way that it does in the EGR system. In the EGR system, CO is injected in the intake manifold to reduce engine emissions. The amount of CO produced by the Econokit however would be insignificant in instigating the effects of EGR. ABT1 0 0 1 85.104 440.35 Tm[(e)4(hou1 271.04 564.50 1 80(stem, C)-3(C

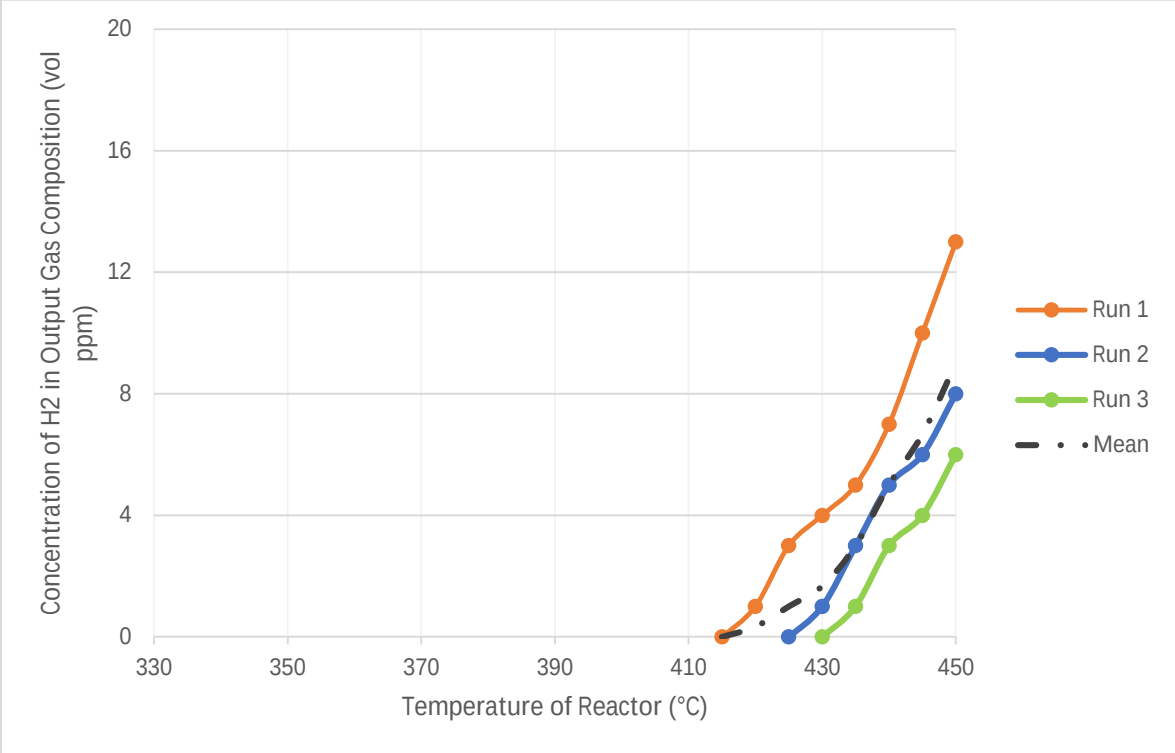

As seen in figure 30 above, at very high temperatures, the reactor also produces H_2. For Run 1, hydrogen was detected from reactor temperature 415 °C, whereas for Run 2 and 3, hydrogen was detected at reactor temperatures 420 °C and 430 °C. Also seen from figure 30 is that when the reactor temperature reached maximum temperature, 450 °C, the concentration of H_2 in the output was 13 ppm, 8 ppm and 6 ppm for Runs 1, 2 and 3 respectively. This shows that even though H_2 is produced in the reactor, the amount produced is minimal and would not have an effect on the engine emissions when injected into the manifold. From the results however, it is also seen that as the temperature is increased, the concentration of H_2 also increases. This indicates that if the reactor temperature is further increased, above 450 °C, there would be a higher concentration of H_2 where it can reach a point where it can be high enough to affect the engine emissions.

If the reactor temperature does increase above 450 °C and the H_2 production becomes sufficient, this will mean that Econokit is injecting H2, CO, CO_2. These three gases are the constituents of syngas, therefore at very high reactor temperatures, the Econokit would be injecting syngas. Syngas when injected would act as a secondary fuel in the combustion chamber [Feng 17]. It assists in combustion, and when injected it would act to reduce PM emissions by achieving more complete combustion and would also act to increase the engine power [Feng 17].

5

References

Arruga, H., Scholl, F., Kettner, M., Amad, O., Klaissle, M. and Giménez, B. (2017). Effect of intake manifold water injection on a natural gas spark ignition engine: an experimental study. *IOP Conference Series: Materials Science and Engineering*, 257, p.012029.

Babu, A., Amba Prasad Rao, G. and Hari Prasad, T. (2015). Direct injection of water mist in an intake manifold spark ignition engine. *International Journal of Automotive and Mechanical Engineering*, 12, pp.2809-2819.

Bureau Veritas (2018). *Efficiency Test of Econokit System*

Tesfa, B., Mishra, R., Gu, F. and Ball, A. (2012). Water injection effects on the performance and emission characteristics of a CI engine operating with biodiesel. *Renewable Energy*, 37(1), pp.333-344.

Tolleson, J. (2018). *US environment agency declares greenhouse gases a threat*. [online] Nature International Weekly Journal of Science. Available at: https://www.nature.com/news/2009/090417/full/news.2009.374.html [Accessed 30 Aug. 2018].

Tschalamoff, T., Laaß, U. and Janicke, D. (2007). Direct water injection in a medium speed gas engine. *MTZ worldwide*, 68(11), pp.15-18.

Union of Concerned Scientists. (2018). *Cars, Trucks, Buses and Air Pollution*. [online] Available

3) Reference chart and table to calculate relative humidity for section 4.4.1 and 5.1

4) Constants used to calculate absolute humidity is section 5.1

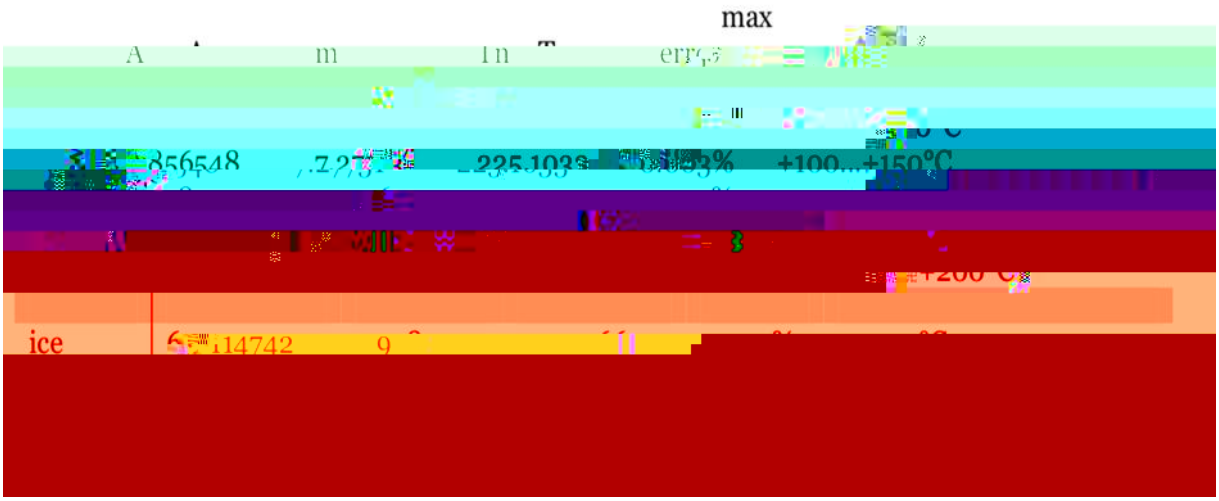

[Vaisala 13]

5) Standard deviation and co-efficient of variance for CO_2 concentration at each reactor temperature (section 5.2.1)

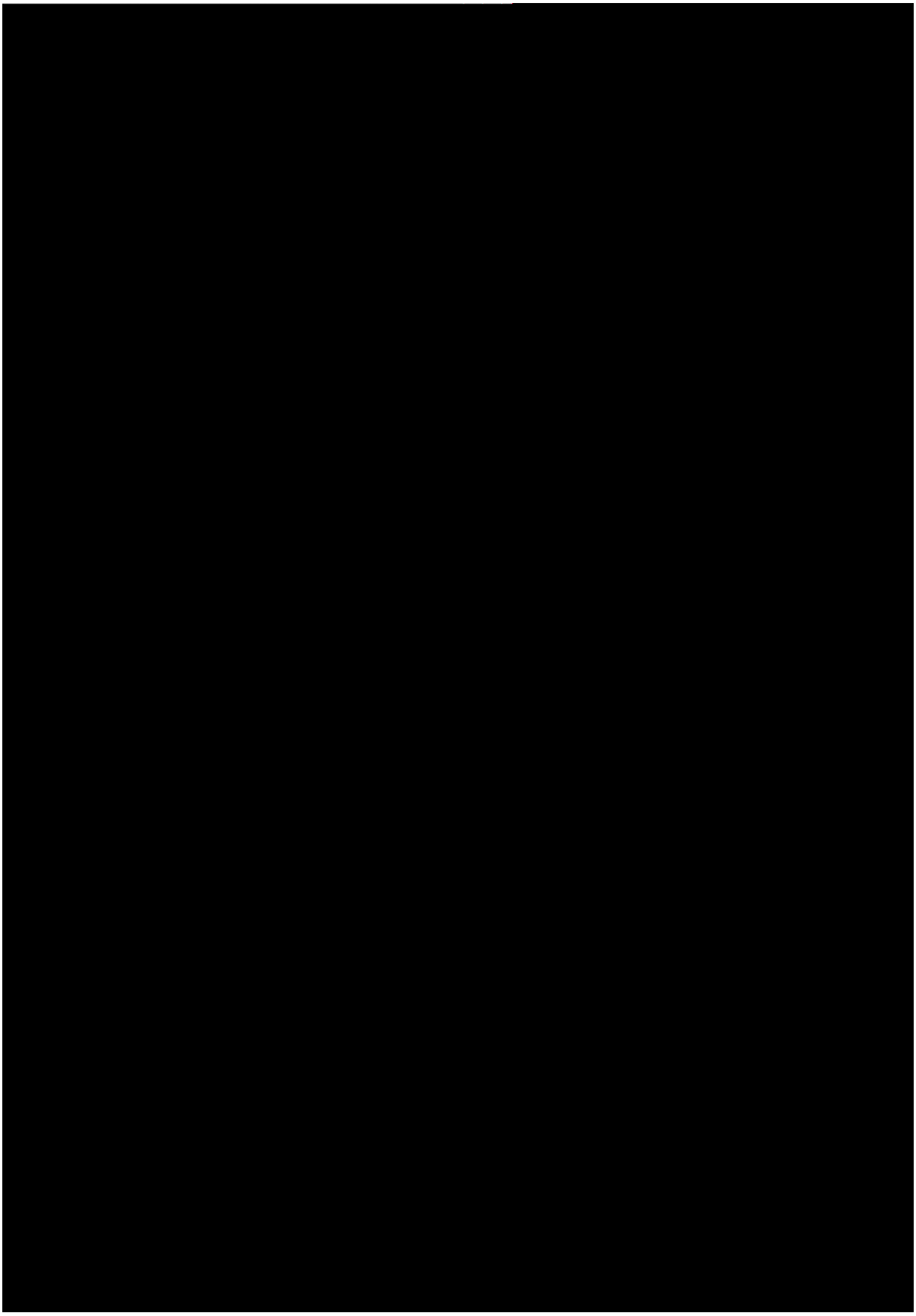

5) Standard deviation and co-efficient of variance for CO concentration at each reactor temperature (section 5.2.2)